ilmedia

TECHNISCHE UNIVERSITÄT
ILMENAU

Weigel, Christoph; Phi, Hai Binh; Denissel, Felix Arthur; Hoffmann, Martin;
Sinzinger, Stefan; Strehle, Steffen

Highly anisotropic fluorine-based plasma etching of ultralow expansion glass

Original published in: Advanced engineering materials. - Weinheim : Wiley-VCH Verl.. - 23 (2021), 6, art. 2001336, 10 pp.

Original published: 2021-02-24

ISSN: 1527-2648

DOI: 10.1002/adem.202001336

[*Visited:* 2022-02-25]

This work is licensed under a Creative Commons Attribution 4.0 International license. To view a copy of this license, visit https://creativecommons.org/licenses/by/4.0/

TU Ilmenau | Universitätsbibliothek | ilmedia, 2022
http://www.tu-ilmenau.de/ilmedia

ADVANCED ENGINEERING MATERIALS
www.aem-journal.com

Check for updates

Highly Anisotropic Fluorine-Based Plasma Etching of Ultralow Expansion Glass

Christoph Weigel, Hai Binh Phi, Felix Arthur Denissel, Martin Hoffmann, Stefan Sinzinger, and Steffen Strehle*

Deep etching of glass and glass ceramics is far more challenging than silicon etching. For thermally insensitive microelectromechanical and microoptical systems, zero-expansion materials such as Zerodur or ultralow expansion (ULE) glass are intriguing. In contrast to Zerodur that exhibits a complex glass network composition, ULE glass consists of only two components, namely, TiO_2 and SiO_2. This fact is highly beneficial for plasma etching. Herein, a deep fluorine-based etching process for ULE 7972 glass is shown for the first time that yields an etch rate of up to 425 nm min^{-1} while still achieving vertical sidewall angles of 87°. The process offers a selectivity of almost 20 with respect to a nickel hard mask and is overall comparable with fused silica. The chemical surface composition is additionally investigated to elucidate the etching process and the impact of the tool configuration in comparison with previously published etching results achieved in Zerodur. Therefore, deep and narrow trenches can be etched in ULE glass with high anisotropy, which supports a prospective implementation of ULE glass microstructures, for instance, in metrology and miniaturized precision applications.

1. Introduction

Ultralow expansion (ULE) glass is a single-phase material and consists of SiO_2 and TiO_2 (here ULE 7972 glass from Corning is used). ULE glass exhibits a long-term dimensional stability without any observable thermal hysteresis[1,2] and is insensitive to temperature changes up to at least 350 °C.[2] Hence, ULE glass can be a material of choice for mask blanks in extreme UV lithography, for substrates in projection optics and in precision metrology, where temperature-stabilized systems with (sub-)nanometer accuracy are required.[3] Notably, most applications for ultra-low expansion materials are so far still linked to macroscopic systems such as mirror substrates in astronomical applications.[4,5]

ULE glasses as well as Zerodur are hitherto rarely used for microscale applications, which originate mainly from a lack of capable manufacturing techniques that provide a superior patterning accuracy and reproducibility at the microscale. For glass (ceramic) machining, conventional processing methods such as surface grinding and polishing or atmospheric pressure plasma jet machining are so far mainly used.[6]

For a pattern transfer in the micrometer scale, methods such as reactive atom plasma etching,[7] femtosecond laser-induced structuring,[8] or ion beam machining[9] are used. These methods exhibit mainly two drawbacks. First, all these methods belong to the group of serial processing methods and second, they can induce structural as well as vibrational changes within the material, if the energy impact is too high.[8] Parallel structuring by wet chemical etching processes appears as an alternative, but the isotropic material properties obstruct an anisotropic structure transfer.

Substrate-based fabrication with an accuracy in a single-digit micrometer range and the respective reproducibility can be achieved by using high-resolution UV lithography and deep reactive ion etching as already demonstrated in complex glass and glass ceramics.[10,11] Nanoimprint techniques in combination with reactive ion etching can be used as well if highly ordered glass nanostructures are targeted.[12]

Vertical sidewalls are particularly important for applications in precision measurement technology. Optically sharp edges of structures can be reached by anisotropic etching, which enhances the overall measuring accuracy and decreases the measurement errors. The ability to create highly anisotropic structures enables furthermore an increase in structural resolution. Vertical sidewalls and high etching depths are fostering the scope of applications. Typical applications comprise, for instance,

Dr. C. Weigel, H. B. Phi, F. A. Denissel, Prof. S. Strehle
Institute of Micro- and Nanotechnologies MacroNano®
Microsystems Technology Group
Technische Universität Ilmenau
Max-Planck-Ring 12, Ilmenau 98693, Germany
E-mail: christoph.weigel@tu-ilmenau.de

Prof. M. Hoffmann
Chair of Microsystems Technology
Ruhr University Bochum
Universitätsstraße 150, Bochum 44801, Germany

Prof. S. Sinzinger
Institute of Micro- and Nanotechnologies MacroNano®
Fachgebiet Technische Optik
Technische Universität Ilmenau
Helmholtzring 1, Ilmenau 98693, Germany

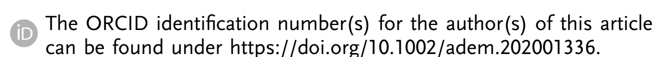
The ORCID identification number(s) for the author(s) of this article can be found under https://doi.org/10.1002/adem.202001336.

© 2021 The Authors. Advanced Engineering Materials published by Wiley-VCH GmbH. This is an open access article under the terms of the Creative Commons Attribution License, which permits use, distribution and reproduction in any medium, provided the original work is properly cited.

DOI: 10.1002/adem.202001336

microfluidics and monolithically integrated optical systems with lateral beam injection.[13]

Recent investigations underlined that the etching of a glass (ceramics) depends strongly on its chemical and structural composition but as well on its thermal properties.[10,11,14] Highly anisotropic etching with almost vertical sidewalls and etch depths larger than 100 μm were demonstrated for fused silica, which can, therefore, serve as a reference.[13] In particular, an etch rate of 300 nm min^{-1} and a selectivity of 20:1 with respect to the nickel hard mask as well as an overall low defect density were achieved. The measured arithmetic mean roughness of the sidewalls was found to be 7 nm, which is suitable for microoptical applications.[13] High etch rates of about 250 nm min^{-1} were achieved for Zerodur too with an etching gas composition of SF_6 or SF_6/Ar, but the sidewall angle was only 71° for the considered processes, which was traced back to nonvolatile reaction products.[11,14] This fact obstructs significantly the achievable aspect ratio of etched structures and thus the reachable etch depth. The amount of nonvolatile reaction products differs for each type of glass. Anticipated reaction products from typical glass components and their respective volatility are shown in **Figure 1** and will be discussed too in detail in the following.

For the aforementioned application scenarios, vertical structures in materials with extremely low thermal expansion are required. The strategy to achieve vertical sidewalls is the use of an appropriate reactive ion etching process and a material that releases only volatile reaction products. Corning's ULE 7972, a titanium silicate glass, is in this regard highly intriguing, as it represents a single-phase, ultralow thermal expansion material with a less complex composition comprising solely SiO_2 and TiO_2.[15] Therefore, ULE 7972 is a promising candidate for a highly anisotropic plasma structuring. For comparison purposes, the glass compositions of ULE 7972 glass, Zerodur, and fused silica are shown in Table S1, Supporting Information.[5] As shown in Figure 1, SiO_2 as well as TiO_2 should both yield volatile reaction products during fluorine-based plasma etching, but only under optimized etching process conditions. The reaction product TiF_4 reaches, for instance, a suitably high vapor pressure at surface temperatures above 100 °C. The maximum surface temperature was measured to be in the range of 110–140 °C. This value was estimated within our studies on a so-called dummy wafer using a process time of 20 min and disposable temperature measurement strips that were protected by Kapton foil. Taking this surface temperature range into account, ULE glass should form exclusively volatile reaction products such as fused silica.

Following the demonstrated glass etching and reaction product considerations, the requirements and expectations for ULE glass patterning can be set in the same range as for fused silica including etch rates in the range of 300 nm min^{-1} with nearly vertical sidewalls and excellent uniformity across the wafer. In this article, we demonstrate that high etch rates, a high selectivity, and vertical sidewalls can be, indeed, achieved for ULE 7972 similar to fused silica within a reactive ion etching process in contrast to the material Zerodur.

2. Experimental Results

2.1. Etch Results of ULE 7972 Glass in Comparison with Zerodur

As mentioned before, plasma etching of fused silica and Zerodur were demonstrated as published elsewhere.[11,13,14] The reported optimized etching conditions served within our studies as the starting point to explore as well the deep etching of ULE 7972 that enabled simultaneously a comparative investigation of the impact of certain material properties. The process parameters used in this article are shown in **Table 1**.

Based on the aforementioned preliminary investigations, processes labeled with (a) in the following represent etching gas mixtures of SF_6/CHF_3 and yielded an optimal structure quality in fused silica, whereas so-called (b) processes represent a gas

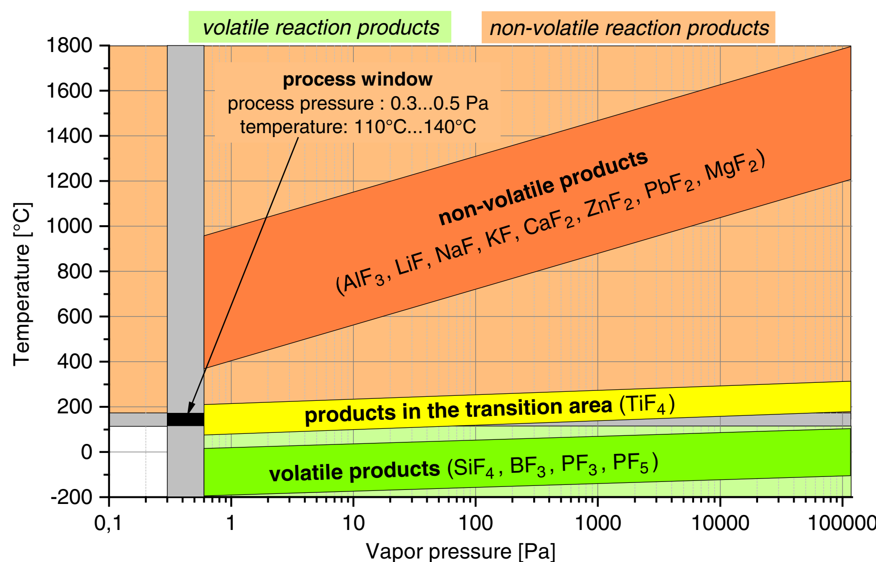

Figure 1. Categorization of certain reaction products that can emerge during the etching of complex glasses into nonvolatiles, volatiles, and products in the transition area.

 © 2021 The Authors. Advanced Engineering Materials published by Wiley-VCH GmbH

Table 1. Process parameters and etch results for the reference process in fused silica (a) and Zerodur EC0 (b) and the transfer to ULE 7972 (c, d) and (e) with an increased ICP power (coolant temperature −10 °C, preset temperature electrode 5 °C, minimal pressure [throttle valve fully open], process time 120 min for Zerodur and ULE and 350 min for fused silica).

Substrate material	Process number	SF_6 [sccm]	CHF_3 [sccm]	Ar [sccm]	ICP [W]	CCP [W]	Bias [V]	Pressure [Pa]	Measured electrode temperature [°C]	Etch rate [nm min^{-1}]	Selectivity	Sidewall angle [°]	R_a etched bottom [nm] (trench width 100 µm)	R_a etched bottom [nm] (large free area (1 × 1) mm^2)
Fused silica	A	15	15	0	500	400[a)]	−350	0.35	35	300	20	88	30	8
Zerodur EC0	B	15	0	15	500	450	−350[a)]	0.27	26	240	8	71	27	10
ULE 7972	C	15	0	15	500	340	−350[a)]	0.36	36	330	15	87	31	20
ULE 7972	D	15	15	0	500	400[a)]	−430	0.39	44	380	26	86	30	14
ULE 7972	E	15	15	0	750	400[a)]	−365	0.42	59	425	19	87	33	12

[a)]Fixed value.

mixture SF_6/Ar and show high etch rates for Zerodur as well as for complex borosilicate glasses. Those optimized processes were applied to titanium silicate glass with only minor adjustments and are labeled in the following with (c) and (d).

Processes labeled with (e) are characterized by an increased inductively coupled plasma (ICP) power of 750 W. The fused silica substrates are comparable with previous work.[13] Using the process parameters shown in Table 1, fused silica, Zerodur, and ULE glass were successfully etched. The results for etch rate, selectivity, and sidewall angle are determined for trench widths of 50 µm. **Figure 2** shows the achieved etch results based on scanning electron microscopy (SEM) images and shows as well the original electroplated nickel structures and the structures directly after the etching.

The roughness of trench bottom with a width of 100 µm was investigated for all processes, as shown in Table 1. For Zerodur, fused silica, and ULE glass, the roughness R_a in the etched trenches is with values between 27 and 33 nm within the same order of magnitude. However, if larger areas of about (1 × 1) mm^2 are inspected, differences between the materials appear. Fused silica shows the lowest roughness for the optimized SF_6/CHF_3 process. The same behavior is found for the ULE glass. A SF_6/Ar mixture results in an increased cratering on the surface for ULE glass, which increases the mean roughness R_a as shown in Figure 2. The same relationship was found for Zerodur.[11] Here, a mean roughness of 6 nm is achieved with an SF_6/CHF_3 gas mixture, whereas a SF_6/Ar gas mixture yields a mean roughness of 10 nm. In principle, any discussion of a surface roughness evolution due to etching requires to consider the etching depth as well, which is, furthermore, linked to the different etching rates. With increasing etch depth, the roughness becomes more pronounced. However, the statement that SF_6/CHF_3 leads to a lower roughness remains unaffected. For all three materials, the investigated R_a value is relatively low and in the same range.

As shown before, fused silica, Zerodur, and ULE glass can be etched in a suitable plasma. However, their respective etch rates and the overall etch performance differ significantly, which is discussed in detail in the following. In **Figure 3**, the etch rates of varied trench widths are depicted. The lines (structure width) and spaces (structure gap) were varied on the mask, as shown in Figure 3.

First, the etch rate of ULE glass was found to be higher compared with Zerodur and even to fused silica. The etch rate is significantly reduced for trenches with a width smaller than 50 µm. This effect can be readily explained by the so-called reactive ion etching lag effect.[16] Figure 3 shows, furthermore, that the relative etch rate reduction in trenches smaller than 20 µm is substantially higher for Zerodur compared with ULE glass and fused silica.

Therefore, differences in the etching angle of ULE glass compared with Zerodur must be taken into account. ULE glass shows nearly vertical sidewalls being in the range of 86–88°, whereas Zerodur etching yielded only a sidewall angle of approximately 71° using the same process parameters. This causes a reduction of the etch rate due to aspect ratio dependent etching effects and results finally in an etch stop. In contrast, ULE glass enables high aspect ratio etching due to its vertical sidewalls. The differences in the etching behavior as well as the sidewall angle are discussed by means of surface chemical investigations in the following section.

The observed increase in the etch rate for ULE glass compared with fused silica can be explained by the different glass networks. Titanium oxide is an intermediate oxide and may therefore act as the so-called network modifier.[17,18] In TiO_2–SiO_2 glass compositions without other network modifiers, titanium incorporates exclusively in fourfold coordination and acts as network former by replacing silicon. This fact leads consequently to a change in the dielectric properties and might be a reason for a slightly different etching behavior compared with fused silica.[17,19] However, the relatively low etch rate of Zerodur in comparison with ULE and fused silica must be explained differently. Zerodur possesses a rather complex material composition, which triggers the generation of a significant quantity of nonvolatile reaction products in a fluorine-based plasma (approximately 36 wt% nonvolatiles for Zerodur).[11] The same is also valid for other complex glass compositions.[10] These nonvolatile products accumulate on the surface and form a stable coating that obstructs the etch progress.

The etch selectivity between glass and the protective nickel mask depends intrinsically on the glass composition and the utilized etching process parameters. The highest selectivity of 26 with respect to the nickel hard mask used here exhibits ULE glass in a SF_6/CHF_3 plasma, which should be based on the reduced

© 2021 The Authors. Advanced Engineering Materials published by Wiley-VCH GmbH

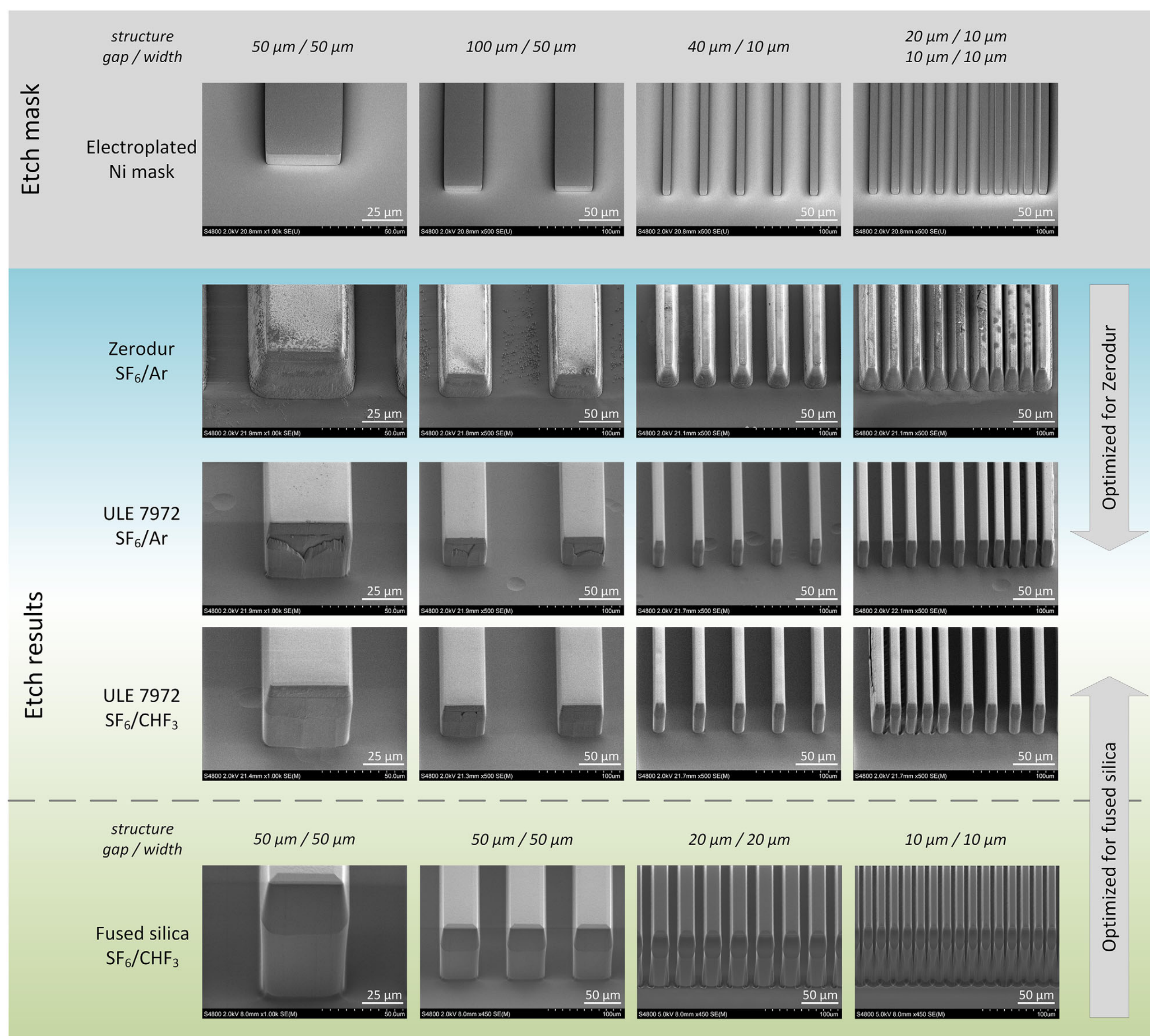

Figure 2. Comparison of structures deep-etched into fused silica, Zerodur EC0, and ULE 7972 glass with varying structure and trench width (direct after the etching process, SEM tilt angle 45°).

physical attack due to the lack of Ar ion bombardment. Nevertheless, Ar addition and the accompanied Ar ion bombardment are so far essential to improve the structuring of complex glass compositions. Ar-induced surface sputtering fosters the removal of nonvolatile products, which have a vapor pressure below the process pressure at typical surface temperatures and can trigger so-called micromasking effects at the surface, as shown, for instance, in the study by Weigel et al.[10,11] Furthermore, the energetic ion bombardment decreases the thickness of the polymer on the surface for an improved physical impact.[20,21] For glasses that form exclusively volatile products such as ULE glass, etching is promoted by CHF_3 addition that yields intrinsically an improved etching behavior.

The plasma density and thus the concentration of reactive species are directly linked to the ICP power. Raising the ICP power increases the chemical reaction by a higher ion flux and a higher density of reactive neutrals due to a higher electron density and thus the etch rate. By increasing the ICP power from 500 to 750 W, respectively, the etch rate for ULE glass increased consequently as well from 380 to 425 nm min^{-1}. However, the enhanced physical and chemical reactions result simultaneously in an increased substrate temperature, which is a critical aspect too considering the thermal mismatch between the glass substrate and the nickel etch mask. Due to the low thermal conductivity of glasses in comparison with, e.g., silicon, an effective cooling is inhibited and the surface temperature is strongly affected by the applied ICP power. For materials with ultralow thermal expansion, the mismatch of thermal expansion between the mask and the substrate can be critical, causing damages such as surface cracks and mask delamination induced by thermal

 © 2021 The Authors. Advanced Engineering Materials published by Wiley-VCH GmbH

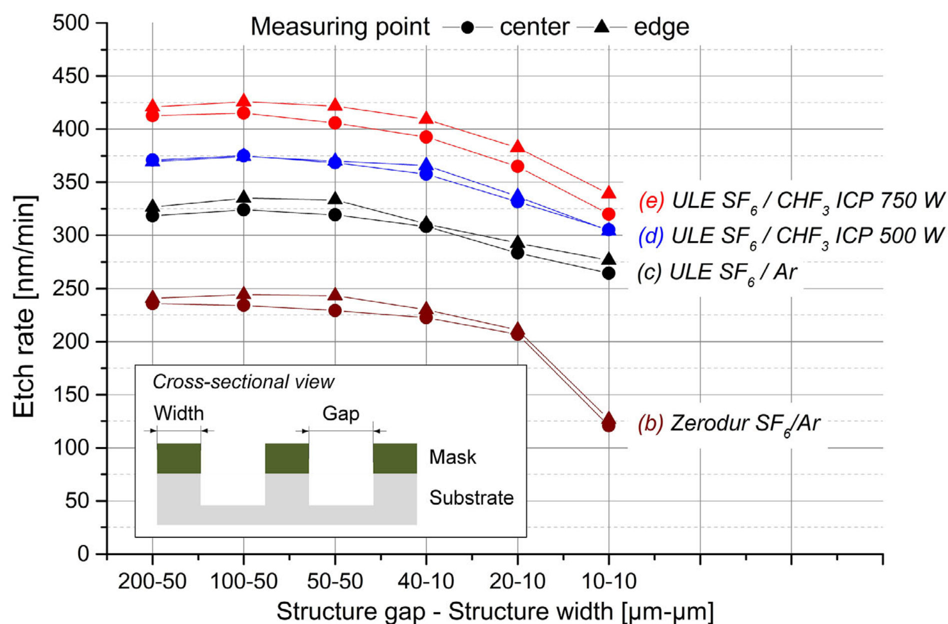

Figure 3. Etching rate depending on material, etching process, structure gap (trench width), and the location on the substrate (wafer center and wafer edge).

stress. This is, in particular, true in the case of structures that shall be freestanding or fully released from the bulk substrate.[14] The thermal load can be reduced aside from a lowered ICP power by implementing cyclic processes with alternating etching and cooling steps. At this point, it should be mentioned that the cooling phases reduce the effective etch rate. Notably, it was observed that a higher ICP power reduces the selectivity between the glass and the nickel mask due to a pronounced nickel etch mask attack (higher ion flux).

2.2. Surface Chemical Investigations

The sidewalls and the bottom of etched features in ULE glass were investigated in comparison with Zerodur by SEM/energy dispersive X-ray (EDX). The required electron acceleration energy for the elemental X-ray excitation was 10 kV, which limits the surface sensitivity due to an enhanced electron penetration depth. Therefore, the EDX results can only serve as an indicator for the composition of the investigated surfaces. The concentration of carbon was set to zero. Thus, the influence of impurities and carbon layers present on the surface is neglected in the elemental surface composition. The SEM/EDX mappings in **Figure 4** show a top view of the etched structures and a direct view on the etched sidewalls (normal direction) of ULE glass and Zerodur.

The deep-etched trenches of ULE glass possess a width of 50 µm and were etched using the SF_6/Ar and SF_6/CHF_3 plasma etching gas composition (c) and (d) as shown in Table 1. The elemental mapping was restricted to the glass composites O, Si, Al, Ti, and the mask material Ni. The glass components were mainly detected on the etched bottom, whereas nickel is located mainly, as expected, on the masked areas but in small amounts also at the etched trench bottom. These are resputtered mask particles caused by the impact of high-energy ions but without any significant impact on the structural quality (e.g., no observable micromasking effect), as shown in Figure 2. The sidewall inspection of the etched ULE glass samples shows, furthermore, the presence of an increased concentration of aluminum. As aluminum is not a component of the glass composition, it is assumed that the source of aluminum compounds is not the material itself but originates from other sources (e.g., machine parts). Machine parts, consisting for instance of Al_2O_3, are exposed to the plasma process too and can thus contribute nonvolatile products in a fluorine-based plasma. A detailed discussion follows in the next section. However, it seems that these contaminations have no critical impact on the sidewall angle and the roughness evolution during etching. Nevertheless, the creation of reaction products and, in particular, of nonvolatiles at the substrate surface during plasma etching is of special interest to understand the overall etching characteristics. This is in the focus of the following discussion.

After the etching process, the removal of the redeposition layer can be realized by wet chemical etching of the masking layer Ni, Au, and TiW with the previously given etchants and by applying a piranha solution as the final step. SEM images of the structures after the etching as well as after the cleaning are shown in **Figure 5**.

3. Discussion

As mentioned before, fused silica consists only of silicon and oxygen unlike Zerodur that exhibits a complex composition consisting of aluminum, alkali metals, earth alkali metals, and further oxides. In comparison, ULE glass offers nearly the same low thermal expansion as Zerodur but is composed only from

 © 2021 The Authors. Advanced Engineering Materials published by Wiley-VCH GmbH

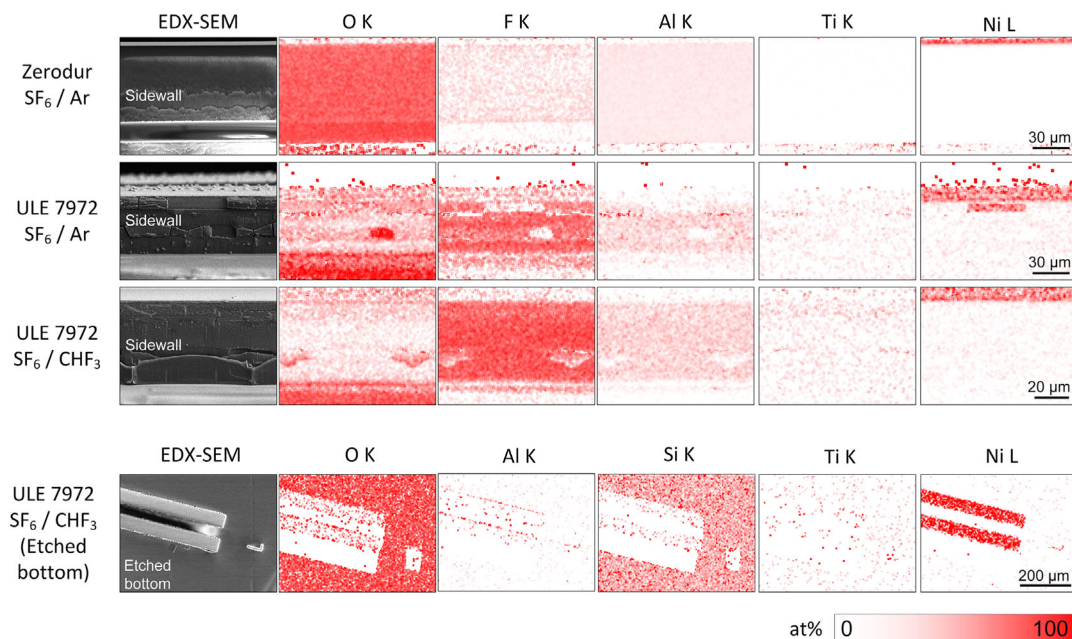

Figure 4. Top section: SEM/EDX investigation of deep-etched sidewalls in Zerodur and ULE glass in SF_6/Ar and SF_6/CHF_3 plasma (incident electron beam angle 90°, acceleration voltage 10 kV); bottom section: SEM image and EDX elemental mappings of the SF_6/CHF_3 etched ULE glass bottom (process number (d) with 500 W ICP power, incident electron beam EDX, acceleration voltage 10 kV).

silicon, oxygen, and titanium, which were accordingly detected by SEM/EDX as shown in Figure 4.

For ULE glass, the concentration of the elements at the etched ground is almost constant before and after plasma etching (Table S2, Supporting Information). This indicates a formation of volatile reaction products without a significant enrichment of single or certain elements at the surface. At the low utilized process pressures, all products are gaseous at the experimentally determined surface temperature (range between 110 and 140 °C; see Figure 1). ULE glass can therefore be etched by reactive ion etching in a fluorine-based plasma with nearly vertical sidewalls and high etch rates, which are comparable with those of fused silica. In comparison with Zerodur, nonvolatile by-products cannot be avoided even by varying the process parameters. This comes from the fact that the process pressure is already quite low and, thus, adequate vapor pressures would require a significant increase in surface temperatures meaning above 700 °C. However, the addition of Ar gas to the etching gas mixture should increase the overall ion flux and lead to an enhanced physical etching (sputtering) of those nonvolatile reaction products. This becomes evident by the nearly constant element concentration that was detected at a pristine surface in comparison with the state after etching (cf. Table S2, Supporting Information).

The sidewalls of the complex glass ceramic Zerodur show an enrichment of Al and F atoms after the etching compared with nonetched Zerodur. These enrichments are either created directly on the sidewall during the etching process or originate from redeposition on the sidewalls based on the fact that physically etched by-products leave the surface in a cosine distribution, as shown in **Figure 6** (right below).[22] As aluminum is a component of the glass ceramic itself, it is not clear whether there is a formation of a thin additional sidewall layer of nonvolatiles or not. The physical interaction of (reactive) ions with the surface enables, in principle, a sufficient removal of nonvolatile reaction products by sputtering and, thus, prevents the formation of thick reaction product layers. The degree of surface layer removal should affect the etching efficiency. Therefore, it is assumed that there is a correlation to the sidewall angle, which is linked to the achievable sputter yield defined by the incidence angle of the ions (see Figure 6, right above).[23] It was found that the highest sputter yield occurs at an ion incident angle of approximately 70°. The resulting sidewall angle of the etched structures thus correlates with the optimum removal of nonvolatile products. Lower angles of ion incidence reduce the sputter yield of nonvolatiles on the sidewall, while larger angles increase the ion reflection from the sidewall. An indicator for a sufficient removal of nonvolatiles is the oxygen concentration, which represent an exposed glass ceramic surface. The absence of a physical etching contribution (e.g., true for geometrically shadowed surfaces) yields a covering layer of nonvolatile reaction products, which inhibits an effective ion-induced chemical etching of the sidewalls.

For ULE glass, an additional layer covers sidewalls of the structures (cf. Figure 4). The layer consists of fluorine and aluminum atoms, while the concentration of oxygen as part of the glass matrix is reduced (Table S2, Supporting Information). Furthermore, a low concentration of approximately 2 at% titanium is detected on the sidewalls. Notably, aluminum is not a component of ULE glass and is, therefore, not expected to be present at the surface as a reaction product of the etching process itself. The most likely reason for the presence of aluminum is the

 © 2021 The Authors. Advanced Engineering Materials published by Wiley-VCH GmbH

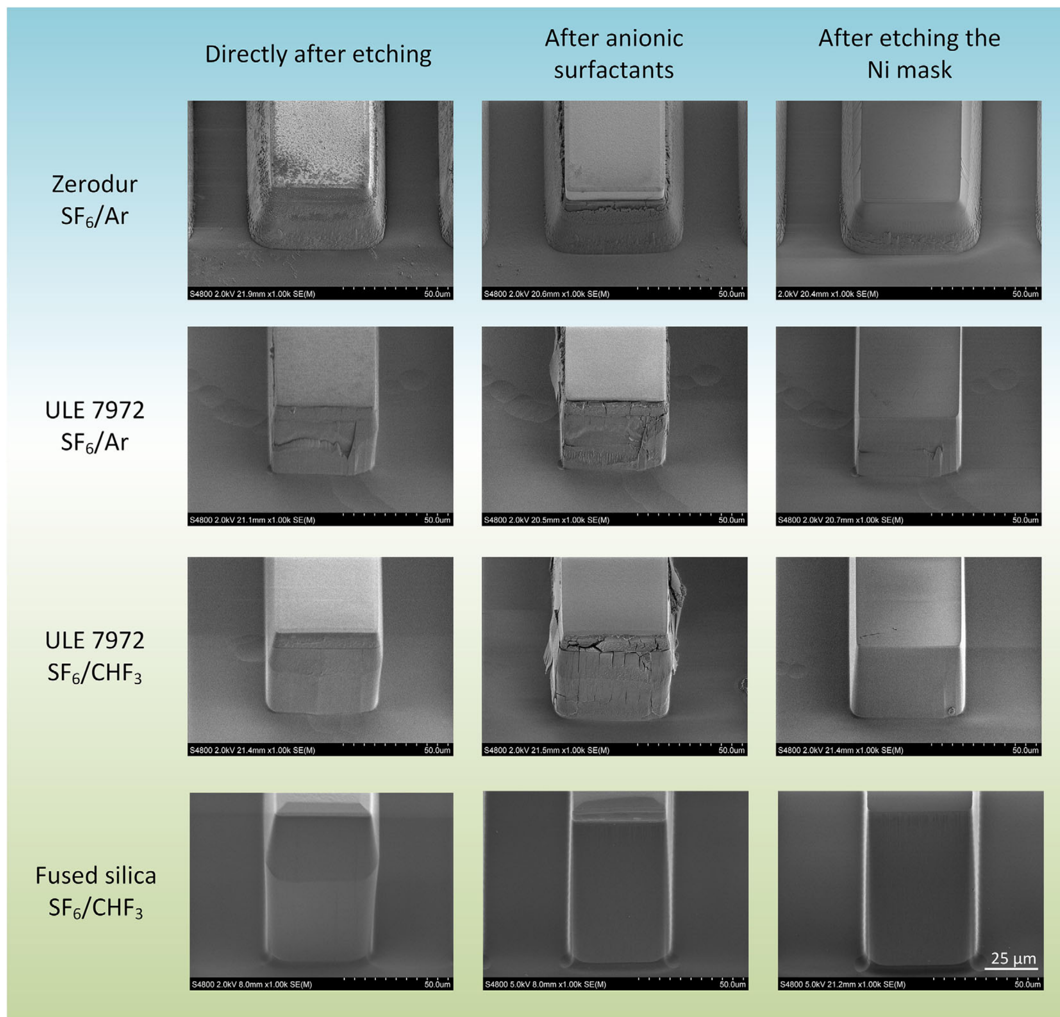

Figure 5. SEM images of etched structures in Zerodur, ULE 7972, and fused silica directly after etching, after the application of anionic surfactants, and after the wet chemical etching of the nickel mask.

tool configuration itself. The substrate wafer is placed on an electrode clamped with an Al_2O_3 carrier (Figure 6). Due to the high ion energy based on an applied bias voltage of −350 V, the clamp-ring is etched too during the plasma etching. The reaction products aluminum and fluorine are sputter-etched and redeposited on the sidewalls of the etched substrate material. The forming of AlF_3 is more likely to the redeposition products than Al_2O_3 because it is more easily sputter-etched.[24] The nearly vertical sidewalls of 86–88° obstruct any significant physical impact of ions to sputter-etch the redeposited products (Figure 6). Thus, an enrichment of aluminum and fluorine atoms occurs on the sidewalls. By using a SF_6/CHF_3 plasma, the simultaneous fluorination of the sidewalls by polymer layers is assumed.[25]

The observed titanium on the sidewalls of the structured ULE glass can be part of the material itself or represent nonvolatile TiF_4 that was formed during etching due to a reduced temperature on the nearly vertical sidewalls by the aforementioned lowered physical ion impact. The hot spot model describes in this regard that a temperature peak occurs at the site of the ion incidence, which favors chemical reactions and converts reaction products into the gas phase.[26] Therefore, the removal of nonvolatiles depends strongly on the surface temperature of the sidewalls.

The created assumptions regarding the generation, removal, and redeposition of nonvolatile reaction products during etching of the different glass materials can also be verified by analyzing the chamber contamination itself. Chamber parts are made of fused silica and were investigated before the manual cleaning procedure. Their contamination depends strongly on the position and orientation inside the chamber. After the etching of various glass samples and glass ceramics, the contamination of the chamber was analyzed at various locations on the chamber components. The measurements are listed in Table S3, Supporting Information, and show that mainly aluminum and fluorine are present. The liner surface contains obviously a maximum concentration of aluminum, as it is perpendicularly oriented to the electric field, which creates hardly any physical

© 2021 The Authors. Advanced Engineering Materials published by Wiley-VCH GmbH

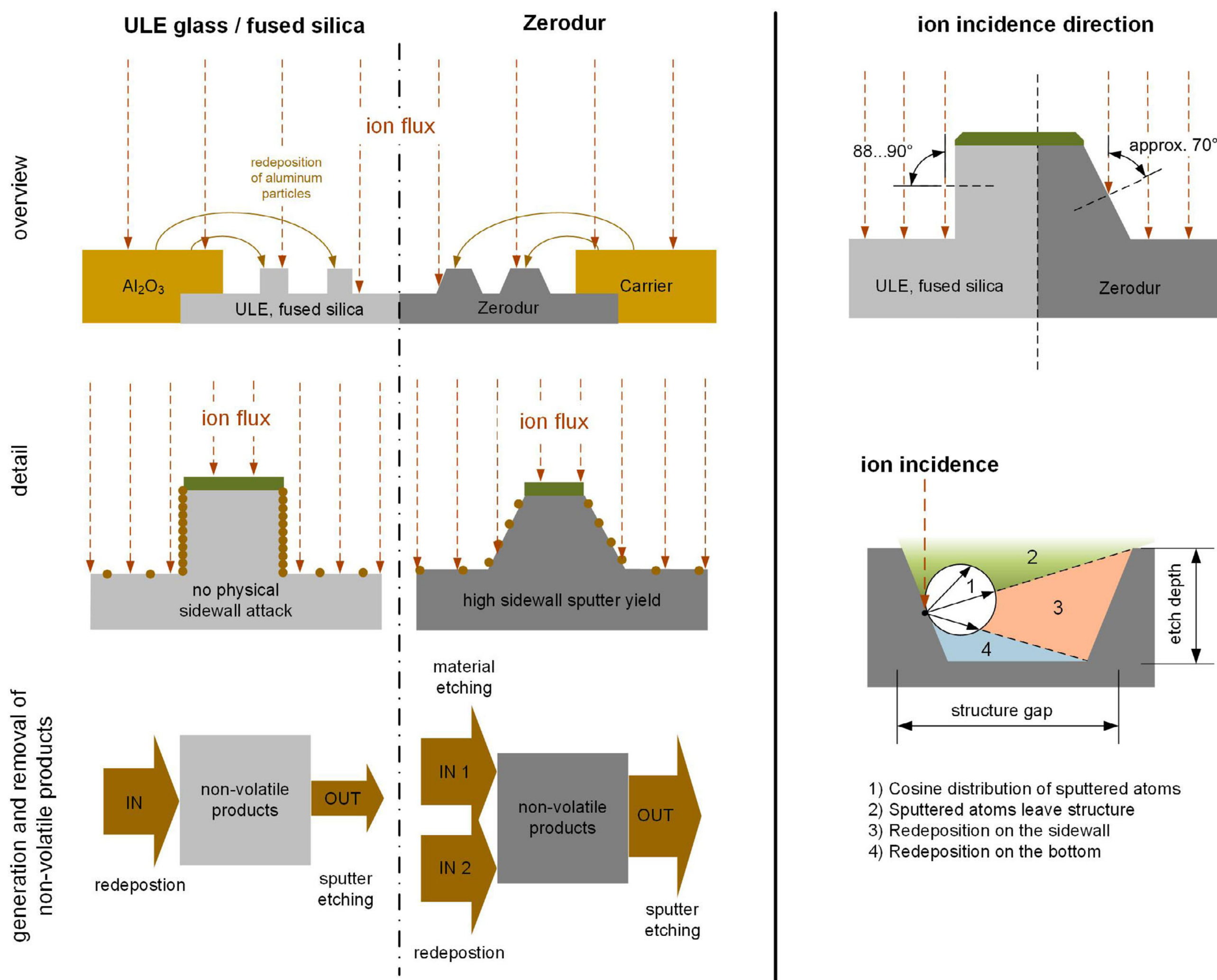

Figure 6. Redeposition and removing of nonvolatile products during etching of different sidewall profiles (left side: IN are nonvolatile products generated by the clamping ring; right side: for Zerodur the nonvolatile products are generated by the clamping ring (IN 1) and by the material itself (IN 2)).

ion bombardment. From the geometrical point of view, this correlates well with the etched sidewalls of ULE glass and fused silica.

In summary, it can be therefore concluded that the redeposition depends not only on the etched material but also on the chamber configuration, as we use a process with high ion energy. It was notably found furthermore, that the sidewalls angle, the etch rate, and the etch selectivity with respect to materials with only volatiles (fused silica, ULE glass) are not altered by these redeposited reaction products. In addition, there is no influence on the roughness of the etched trench bottom due to the so-called micromasking. The physical energy suffices to remove these types of contamination from the etched trench bottom. Moreover, no trenching along the sidewalls was observed. The composition and chemistry of the substrate material itself is the key element that governs the finally achieved structural morphology. The effect of other sources of nonvolatile reaction products (e.g., chamber configuration) plays a subordinate role.

4. Conclusion

The deep fluorine-based plasma etching of low thermal expansion ULE glass, as an alternative to Zerodur, was investigated. Nearly vertical sidewalls were achieved in a fluorine-based plasma, which is a significant advantage in comparison with Zerodur glass ceramics and other complex glasses that enable under similar etching conditions sidewall angles of only 71°. Thus, high aspect ratio structures with small trench width of about 10 μm and below can be realized. Etch rates of 330 and 380 nm min^{-1} and selectivities of 15 and 26 with respect to the nickel mask were achieved by applying structuring processes previously optimized for Zerodur and fused silica. This is a significant improvement in comparison with Zerodur too (maximum etch rate of about 240 nm min^{-1} and selectivity of 8) and with fused silica (etch rate of 300 nm min^{-1} and selectivity of 20) and indicates an improved ability to structure ULE at the used process conditions. The best results with respect to etch rate and selectivity were achieved within the set of analyzed processes

 © 2021 The Authors. Advanced Engineering Materials published by Wiley-VCH GmbH

using a SF_6/CHF_3 plasma at an ICP power of 500 W. These are the same process conditions that were previously used for the anisotropic deep etching of fused silica for microoptical applications.

The implemented structuring process enables, thus, high aspect ratios at high selectivity. This is, for instance, highly beneficial for applications aiming for the final release of microstructures. For Zerodur, a double-sided process for releasing micromechanical elements is so far required due to limited sidewall angle and selectivity, which can be omitted in future by shifting to ULE glass.

Furthermore, the chemical composition of the sidewall and the etched trench bottoms were analyzed. We found on etched sidewalls a significant amount of fluorine and aluminum that are both not part of the original ULE glass composition. While fluorine originates from the etching gas composition, the source of aluminum was traced back to the tool configuration.

Nevertheless, for materials with volatile etching products, the sidewall angle and the etch rate are hardly influenced by such a contamination. The trench bottoms showed, furthermore, no significant enrichment of fluorine and aluminum due to the high ion impact. In summary, we can conclude that highly anisotropic plasma-based structuring of ULE glass is possible at a comparable quality level to fused silica.

5. Experimental Section

Substrate Preparation: In this work, 500 µm thick and 100 mm in diameter wafers of Zerodur with the expansion class 0 (EC0), ULE 7972, and fused silica were used.[15,27] The process flow of the main fabrication steps is shown in Figure S1, Supporting Information, and is similar to process flows published previously elsewhere.[11,13]

All substrates were first cleaned with anionic surfactants to remove adhering particles and other residuals from the surface. UV lithography and nickel electroplating were used to create a suitable 17 µm-thick hard mask with high adhesion and chemical stability that withstands the harsh environment during the plasma etching process. The plasma etching was subsequently performed in an inductively coupled plasma (ICP)–reactive ion etching (RIE) tool (Sentech Si-500).[13] Anionic surfactants were used to remove the layer present on the etched sidewalls after the plasma etch. The removal of the nickel hard mask was achieved by wet etching for 2 h using an iron-(III)-chloride and ammonium persulfate etchant at a temperature of 40 °C. For gold etching, a commercial potassium iodide-based gold etchant with additives compatible with nickel was used.[28] The titanium–tungsten layer was subsequently removed by using a hydrogen peroxide solution (40 vol%) at a temperature of 40 °C for approximately 1 min. The samples were finally rinsed in a mixture of sulfuric acid and hydrogen peroxide (Caro's acid) to remove any residual contaminations.

Analysis Methods: SEM images were captured using a Hitachi S4800 at a tilt angle of 45° for improved 3D impression of the etched structures at constant magnification. For the EDX analysis, a Thermo SDD-Detector System NORAN7 was utilized. The incident angle was set to 90° to maximize the number of counts and therefore the overall signal-to-noise ratio. The electron acceleration voltage varies between 5 and 30 kV, which allowed controlling the surface sensitivity for the compositional characterization.

Etch depth measurements were performed using an optical microscope at an optical magnification of 1000×. The etch depth measurement was achieved by setting the focus plane to the top of the mask and subsequently to the bottom of an adjacent etched structure. The measurement was realized with an incremental encoder installed at the microscope with a resolution of 0.1 µm. As both the measured etching depths and the mask thickness are in the range of more than 15 µm, the error is in the range of about ±1%.

To determine the etch selectivity, measurements of the initial mask thickness as well as of the achieved etch depth with and without mask are required. Intermediate measurements of etch depths during extended etching processes should not be used as a quantitative assessment because the remaining thickness of the etch mask can only be determined once the etching process is finished. For the interpolation, the actual mask thickness and the selectivity determined in previous work were here implemented.[11] For the final characterization, all additional layers and the polymer coatings were removed to avoid parasitic effects. The sidewall angle was calculated using the measured trench width at the top and on the bottom while considering the measured etching depth. The mean arithmetic roughness R_a of the etched surface (trench bottom) was measured using a white light interferometer microscope (Veeco Wyko NT9300) within trench widths of 100 µm and larger areas of (1 × 1) mm^2.

Supporting Information

Supporting Information is available from the Wiley Online Library or from the author.

Acknowledgements

Funding of this work through internal funds of the Technische Universität Ilmenau is gratefully acknowledged. The authors thank, furthermore, Shuhao Si, Christian Koppka, Henry Romanus, David Venier, Birgitt Hartmann, and Joachim Döll from the Technische Universität Ilmenau for their experimental support.

Open access funding enabled and organized by Projekt DEAL.

Conflict of Interest

The authors declare no conflict of interest.

Keywords

fluorine plasma, glass etching, ICP-RIE, plasma etching, ultralow expansion glass

Received: November 6, 2020
Revised: February 15, 2021
Published online: March 11, 2021

[1] a) J. W. Pepi, D. Golini, *Appl. Opt.* **1991**, *30*, 3087; b) S. C. Wilkins, D. N. Coon, J. S. Epstein, in *32nd Annual Int. Technical Symp. on Optical and Optoelectronic Applied Science and Engineering 1988* (Ed.: A. J. Marker), SPIE, San Diego, CA **1989**.
[2] J. J. Shaffer, H. E. Bennett, *Appl. Opt.* **1984**, *23*, 2852.
[3] a) K. E. Hrdina, C. A. Duran, *Int. J. Appl. Glass Sci.* **2014**, *5*, 82; b) G. Jäger, E. Manske, T. Hausotte, A. Müller, F. Balzer, *Surf. Topogr.: Metrol. Prop.* **2016**, *4*, 34004; c) E. Manske, G. Jäger, T. Hausotte, R. Füßl, *Meas. Sci. Technol.* **2012**, *23*, 74001; d) S. Hartlieb, M. Tscherpel, F. Guerra, T. Haist, W. Osten, M. Ringkowski, O. Sawodny, *tm – Technisches Messen* **2020**, *87*, 504.
[4] a) Y. X. Yao, B. Wang, J. H. Wang, H. L. Jin, Y. F. Zhang, S. Dong, *CIRP Ann.* **2010**, *59*, 337; b) W. Arens, V. Schmidt, *Photonik* **2004**, *36*, 56; c) W. Pannhorst, *Spektrum der Wissenschaft* **1993**, *11*, 102.
[5] a) H. A. Schaeffer, R. Langfeld, *Werkstoff Glas: Alter Werkstoff mit großer Zukunft*, Springer Berlin Heidelberg, Berlin, Heidelberg **2014**; b) R. Sabia, M. J. Edwards, R. VanBrocklin,

 © 2021 The Authors. Advanced Engineering Materials published by Wiley-VCH GmbH

B. Wells, in *Optomechanical Technologies for Astronomy 2006* (Eds: E. Atad-Ettedgui, J. Antebi, D. Lemke), SPIE, Orlando, FL **2006**.
[6] P. A. Pawar, R. Ballav, A. Kumar, in *Int. Conf. on Fibre Optics and Photonics 2016*, OSA Technical Digest, Kanpur, India **2016**.
[7] a) T. Arnold, G. Böhm, H. Paetzelt, in *Advances in Optical and Mechanical Technologies for Telescopes and Instrumentation II* (Eds.: R. Navarro, J. H. Burge), SPIE, Edinburgh, UK **2016**; b) C. Fanara, P. Shore, J. R. Nicholls, N. Lyford, J. Kelley, J. Carr, P. Sommer, *Adv. Eng. Mater.* **2006**, *8*, 933.
[8] I. Efthimiopoulos, D. Palles, S. Richter, U. Hoppe, D. Möncke, L. Wondraczek, S. Nolte, E. I. Kamitsos, *J. Appl. Phys.* **2018**, *123*, 233105.
[9] D. M. Allen, P. Shore, R. W. Evans, C. Fanara, W. O'Brien, S. Marson, W. O'Neill, *CIRP Ann.* **2009**, *58*, 647.
[10] C. Weigel, S. Sinzinger, M. Hoffmann, in *20th Int. Conf. on Solid-State Sensors, Actuators and Microsystems & Eurosensors XXXIII (TRANSDUCERS & EUROSENSORS XXXIII)*, IEEE, Piscataway, NJ **2019**.
[11] C. Weigel, M. Schulze, H. Gargouri, M. Hoffmann, *Microelectron. Eng.* **2018**, *185–186*, 1.
[12] S. Si, C. Weigel, M. Messerschmidt, M. W. Thesen, S. Sinzinger, S. Strehle, *Micro Nano Eng.* **2020**, *6*, 100047.
[13] C. Weigel, E. Markweg, L. Müller, M. Schulze, H. Gargouri, M. Hoffmann, *Microelectron. Eng.* **2017**, *174*, 40.
[14] C. Weigel, S. Sinzinger, M. Hoffmann, *Microelectron. Eng.* **2018**, *198*, 78.
[15] Corning, ULE® Corning Code 7972 Ultra Low Expansion Glass: Datasheet 2008, https://www.corning.com/media/worldwide/csm/documents/D20FD2EA-7264-43DD-B544-E1CA042B486A.pdf (accessed: December 2019).
[16] R. A. Gottscho, C. W. Jurgensen, D. J. Vitkavage, *J. Vac. Sci. Technol. B* **1992**, *10*, 2133.
[17] G. S. Henderson, *Can. Mineral.* **2005**, *43*, 1921.
[18] F. Farges, G. E. Brown, A. Navrotsky, H. Gan, J. J. Rehr, *Geochim. Cosmochim. Acta* **1996**, *60*, 3039.
[19] G. S. Henderson, M. E. Fleet, *J. Non-Cryst. Solids* **1997**, *211*, 214.
[20] a) K. Morikawa, K. Matsushita, T. Tsukahara, *Anal. Sci.* **2017**, *33*, 1453; b) T. Ichiki, Y. Sugiyama, T. Ujiie, Y. Horiike, *J. Vac. Sci. Technol. B* **2003**, *21*, 2188.
[21] J. H. Park, N.-E. Lee, J. Lee, J. S. Park, H. D. Park, *Microelectron. Eng.* **2005**, *82*, 119.
[22] M. Küstner, W. Eckstein, V. Dose, J. Roth, *Nucl. Instrum. Methods Phys. Res., Sect. B* **1998**, *145*, 320.
[23] P. Sigmund, in *Sputtering by Particle Bombardment I: Physical Sputtering of Single-Element Solids* (Ed.: R. Behrisch), Springer Berlin Heidelberg, Berlin, Heidelberg **1981**, p. 9.
[24] D.-M. Kim, M.-R. Jang, Y.-S. Oh, S. Kim, S.-M. Lee, S.-H. Lee, *Surf. Coat. Technol.* **2017**, *309*, 694.
[25] N. R. Rueger, J. J. Beulens, M. Schaepkens, M. F. Doemling, J. M. Mirza, T. E. F. M. Standaert, G. S. Oehrlein, *J. Vac. Sci. Technol. A* **1997**, *15*, 1881.
[26] K. Nojiri, *Dry Etching Technology for Semiconductors*, Springer, Cham, Heidelberg, New York **2015**.
[27] A. G. Schott, *Zerodur: Zero Expansion Glass Ceramic 2011*, https://www.schott.com/d/advanced_optics/f7ae3c11-0226-4808-90c7-59d6c8816daf/1.3/schott_zerodur_katalog_july_2011_en.pdf (accessed: November 2018).
[28] Sigma-Aldrich, *Gold etchant, nickel compatible | Sigma-Aldrich 2016*, http://www.sigmaaldrich.com/catalog/product/aldrich/651842?lang=en®ion=US (accessed: December 2016).

 © 2021 The Authors. Advanced Engineering Materials published by Wiley-VCH GmbH